

# Magnus Carlsen Takes Flight

Group: *Checkmate*

Matthew Ahern, Sam Burns, Guilherme Jardim, Seojoon Kwon

December 1st 2023



## Nomenclature

- AR: Aspect Ratio
- b: Wingspan (m)
- c: Mean Chord (m)
- $c_d$ : Drag Coefficient of a 2D Wing
- $C_D$ : Drag Coefficient of a Finite Wing
- $C_{D,i}$ : Induced drag coefficient (wing only)
- $C_{D,0}$ : Parasitic Drag Coefficient
- $c_l$ : Lift coefficient of a 2D Wing
- $C_L$ : Lift coefficient of a Finite Wing
- $c_{l,\alpha}$ : 2D Lift Slope
- $C_{L,\alpha}$ : Lift Slope of a Finite Wing
- $D$ : Drag Force (N)
- $D_i$ : Induced Drag Force (wing only) (N)
- $e_v$ : Oswald Efficiency
- $K$ : Fitting Coefficient, equal to  $\frac{1}{\pi e_v AR}$
- $L$ : Lifting Force (N)
- $q$ : Dynamic Pressure, equal to  $\frac{1}{2}\rho U^2 \frac{N}{m^2}$
- $S$ : Wing Planform Area ( $m^2$ )
- $S_w$ : Wetted Surface Area ( $m^2$ )
- $U$ : Flight speed ( $\frac{m}{s}$ )
- $\alpha$ : Angle of Attack (AOA) ( $^\circ$ )
- $\gamma$ : Glide slope ( $^\circ$ )
- $\nu$ : Kinematic Viscosity of air at sea level, equal to  $1.5 \times 10^{-5}(\frac{m^2}{s})$

# 1 Introduction

## 1.1 The Basic Equations of Flight Mechanics

Aerodynamics is a remarkable field, revealing the intricate patterns in which solids move through the air. For all aircraft, including a glider like *Checkmate*, even the most basic equations can offer a powerful way to predict and model flight. In gliding flight, the lift and drag forces create 2 clear sections which can be used to derive these basic, yet governing equations.

### Understanding the Basic Equations: Drag and Lift

Prior to defining equations with tangible results, there are several basic equations of flight mechanics which must be defined. The section below will be dedicated to defining such that.

#### 1. Lift

$$L = qSC_L \quad (1)$$

The lift equation shows a simple relationship between the coefficient of lift, the dynamic pressure, the wing area, and the lifting force.  $C_L$ , the finite lift coefficient, is determined through a calculation using  $c_l$ , the 2D section lift coefficient, and the aspect ratio,  $AR$ .

It is extremely difficult to manually calculate the  $c_l$  of an airfoil. An accurate way to determine *Checkmate's*  $c_l$  is by identifying a similarly-shaped NACA airfoil, based on maximum camber, distance of maximum camber and thickness, all as percent of the chord. Then it is simple to evaluate the already simulated polars. NACA 6412 is the closest airfoil to *Checkmate's* airfoil. The  $\alpha_{0L}$  is determined by identifying the  $\alpha$  when  $c_l = 0$  on the pre-simulated NACA 6412  $c_l$  versus  $\alpha$  polar.

$$C_{L,\alpha} = \frac{2\pi(AR)}{(AR) + 2} \quad (2)$$

$C_{L,\alpha}$  describes the rate of change in  $C_L$  based on  $\alpha$  in radians. Considering that  $C_L = 0$  when  $c_l = 0$ , and that  $C_L$  increases linearly with an increase in  $\alpha$ , the  $C_L$  at the set angle of attack of  $2^\circ$  can be found.

$$C_L = \frac{dC_L}{d\alpha}(\alpha_{0L} - \alpha) \quad (3)$$

#### 2. Drag

The total drag,  $D$ , of the aircraft consists of the aircraft parasitic drag,  $D_0$ , and the lift-induced drag,  $D_i$ .

$$D = D_0 + D_i \quad (4)$$

The parasitic drag  $D_0$  consists of  $D_f$ , the friction drag from non-lifting surfaces of the plane, and  $D_{pro}$ , the profile drag of the wing.

$$D_0 = D_f + D_{pro} \quad (5)$$

$D_f$  accounts for friction acting on the fuselage, horizontal stabilizer, and vertical stabilizer. Each section has a

designated friction coefficient  $C_f$ , and a wetted surface area  $S_w$ .

$C_f$  is determined using the Reynolds Number based on length ( $Re_l$ ), and the ( $Re_l$ ) flow-wise length of the surface ( $l$ ).

$$Re_l = \frac{ul}{\nu} \quad (6)$$

$$C_f = \frac{1.328}{\sqrt{Re_l}} \quad (7)$$

$C_f$  and  $S_w$  can be used to find  $D_f$ .

$$D_f = q(S_{w,fus}C_{f,fus} + S_{w,VS}C_{f,VS} + S_{w,HS}C_{f,HS}) \quad (8)$$

Next, the profile drag  $D_{pro}$  is calculated using the minimum drag coefficient of the airfoil ( $c_{d,min}$ ), dynamic pressure  $q$ , and wing section area  $S$ .  $c_{d,min}$  is found using the airfoil geometry of NACA 6412 at  $Re = 5 \times 10^4$ . Using  $c_{d,min}$  and  $S$ ,  $D_{pro}$  can be determined.

$$D_{pro} = c_{d,min}qS \quad (9)$$

The last component of drag is the induced drag,  $D_i$ .

$$D_i = C_{D,i}qS \quad (10)$$

It can also be found that:

$$C_{D,i} = KC_L^2 \quad (11)$$

$K$  is a constant consisting of the aspect ration  $AR$  and the Oswald efficiency number  $e_v$ .

$$K = \frac{1}{\pi e_v AR} \quad (12)$$

From a derivation of Equation 1, it can be demonstrated that

$$C_L^2 = \frac{L^2}{(qS)^2} \quad (13)$$

If the plane is in steady, level flight, ( $L = W$ ), substituting Equations 11, 12, and 13 into Equation 10 brings the following result:

$$D_i = \frac{KW^2}{qS} \quad (14)$$

## Gliding Flight

From the components of force affecting the movement of the aircraft, the specific type of flight of *Checkmate* can be defined: gliding flight. In ideal gliding flight, the aircraft has no thrust, and all forces are in equilibrium. In the case of this report, *Checkmate* is assumed to glide down at a constant airspeed and sink rate.

## 1.2 Predictions and Measurable Quantities

To measure and predict the flight of *Checkmate*, the following quantities can be utilized:

- L: Lifting forces on the glider
- D: Drag forces on the glider
- W: Weight of the glider
- $\gamma$ : Angle from horizontal line to direction of airspeed

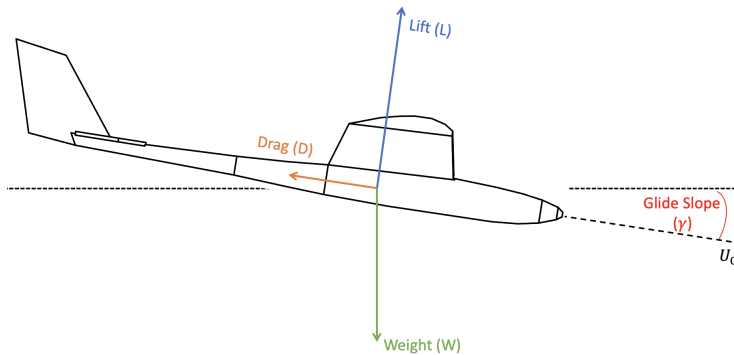


Figure 1: Free Body Diagram of a Gliding Plane

As mentioned in Section 1.1, the horizontal and vertical forces remain in equilibrium during flight. The following force equations can be formed using the forces in Figure 1:

$$L = W \cos(\gamma) \quad (15)$$

$$D = W \sin(\gamma) \quad (16)$$

Equation 15 and 16 can now be used to derive the maximum range of *Checkmate*.

$$\frac{D}{L} = \frac{\sin(\gamma)}{\cos(\gamma)} \quad (17)$$

Therefore,

$$\tan(\gamma) = \frac{1}{\frac{L}{D}} \quad (18)$$

From Equation 18, it can be seen that  $(\frac{L}{D})_{max}$ , the highest achievable ratio between lift and drag, occurs at  $\gamma_{min}$ .

Additionally, with the assumptions of gliding flight mentioned in Section 1.1, the following can be found:

$$\tan(\gamma) = \frac{h}{R} \quad (19)$$

Combining Equations 18 and 19, the following relationship between the  $\frac{L}{D}$  ratio, height, and range can be found.

$$\frac{R}{h} = \frac{L}{D} \quad (20)$$

From Equation 20, the equation for maximum range can be constructed

$$R_{max} = h \left( \frac{L}{D} \right)_{max} \quad (21)$$

The objective of the predictions is to estimate  $R_{max}$  and the flight speed  $U$  at which  $R_{max}$  occurs. With the derivations from Section 1.1 and Section 1.2, and with known constant parameters,  $\frac{L}{D}$  at a certain flight speed  $U$  can be calculated.

For simplicity of calculation,  $\cos(\gamma) \simeq 1$  at low  $\gamma$ . Therefore:

$$L = W \quad (22)$$

Next, drag  $D$  needs to be calculated in terms of  $U$ .  $D$  consists of the two components specified in Section 1.1,  $D_0$  and  $D_i$ . As shown in Equation 4,  $D_0$  consists of  $D_f$  and  $D_{pro}$ . The relationship between  $D_f$  and  $U$  can be found with Equation 8.

$$D_f \sim q \sim U^2 \quad (23)$$

The relationship between  $D_{pro}$  and  $U$  can be found with Equation 8.

$$D_{pro} \sim q \sim U^2 \quad (24)$$

The relationship between  $D_0$  and  $U$  can be seen to be:

$$D_0 \sim U^2 + U^2 \sim U^2 \quad (25)$$

The relationship between  $D_i$  and  $U$  can be determined with Equation 14:

$$D_i \sim \frac{1}{q} \sim \frac{1}{U^2} \quad (26)$$

Then,  $\left(\frac{L}{D}\right)_{max}$  can be located over the flight speed range. Since it can be deduced that  $R$  is directly proportional to  $\frac{L}{D}$  with constant launch height  $h$ ,  $R_{max}$  can be found with  $\left(\frac{L}{D}\right)_{max}$ . With all other parameters of drag being held constant except for airspeed  $U$ , and since  $L = W$ ,  $\frac{L}{D}$  can be plotted over various air speeds to find  $\left(\frac{L}{D}\right)_{max}$ . With a known  $\left(\frac{L}{D}\right)_{max}$  and launch height  $h$ ,  $R_{max}$  can be predicted at a specified airspeed.

During flight test, the predicted maximum range and airspeed are tested. The explanation of the testing procedure is continued in Section 2.

## 2 Materials and Methods

### 2.1 Glider

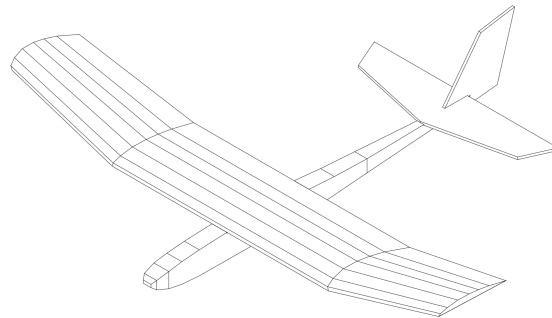


Figure 2: CAD Model of *Checkmate*, Drawn From Online Plans

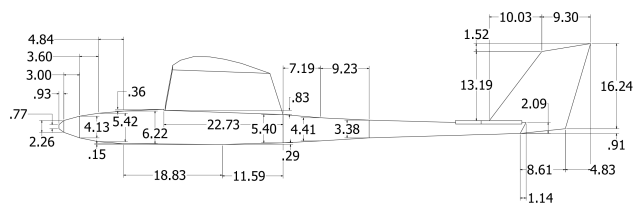


Figure 3: Annotated Side View of *Checkmate* (dimensions in cm)

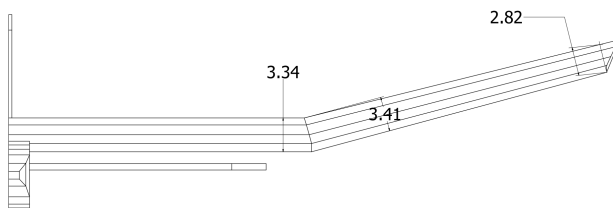


Figure 4: Annotated Front View of *Checkmate* (dimensions in cm)

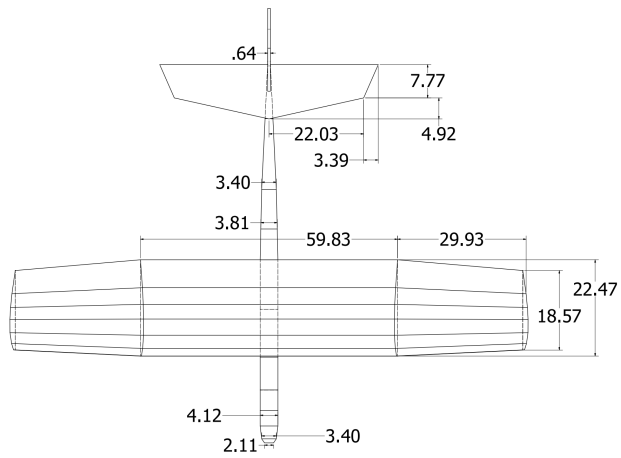


Figure 5: Annotated Top View of *Checkmate* (dimensions in cm)

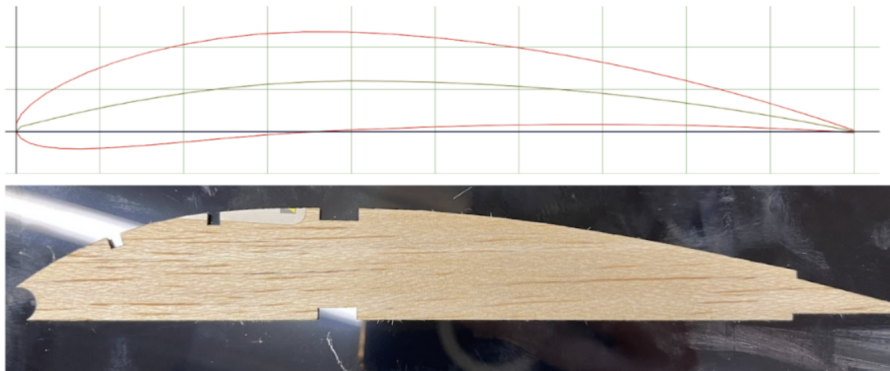


Figure 6: Geometrical Comparison Between NACA6412 (Above) and Airfoil Used (Below)

Measurement	Value
Tip to tip span (b)	1.27m
Planform Area (S)	0.296m <sup>2</sup>
MAC ( $\bar{c}$ )	0.231m
AR	5.5
Maximum Thickness	12%
Maximum Camber	6%
Leading Edge to Max Camber	37%
Airfoil Used	NACA 6412

Table 1: *Checkmate*'s Dimensions

## 2.2 Testing Procedures

*Checkmate* took flight for the first time just after 6am. Flying in the early morning minimized winds, which tend to increase when the sun is out. A special launching apparatus was used to launch the gliders at constant height (measured to be 1.58m off the ground) and at precise speeds. Following each one of *Checkmate's* several flights, the speed, horizontal distance from the launch point, X, and the horizontal distance perpendicular to the launch direction, Y were all recorded. The total length of each flight path, R, can be estimated using the  $\sqrt{X^2 + Y^2}$ , assuming that the flight path was a straight line.

Term	Definition	Evaluation Method	Value
X	Measured Horizontal Distance From Launch Point	Surveyor's Tape Measure	Varies
Y	Measured Horizontal Distance Perpendicular to Launch Direction	Surveyor's Tape Measure	Varies
h	Launch Rail Height	Measuring Tape	1.58 m
R	Range (Total Length of Flight Path)	$R = \sqrt{X^2 + Y^2}$	Varies
m	Mass of Glider	Scale	0.550 kg
T	Atmospheric Temperature	Cellphone Weather App	288 K
$U_0$	Launch Speed	Gauge on Launcher	Varies
$p$	Barometric Pressure	Cellphone Pressure Sensor	$1.02(10^5) \frac{N}{m^2}$
$\rho$	Air Density	$\frac{p}{RT}$ , where R is ideal gas const.	$1.23 \frac{kg}{m^3}$
t	Flight Duration	$\frac{R}{U_0}$	Varies

Table 2: Quantities Found in Testing

## 3 Results

### 3.1 Reynolds Number and Drag Estimates

$U = 5 \frac{m}{s}$ ,  $\rho = 1.23 \frac{kg}{m^3}$ ,  $\nu = 1.5 \times 10^{-5} \frac{m^2}{s}$ , Assuming flow is laminar as  $Re < 5 \times 10^5$

Component	Length (m)	$Re_l = \frac{Ul}{\nu}$	$C_{f,Component} = \frac{1.328}{\sqrt{Re_l}}$	$S_{w,Component} (m^2)$
Fuselage, fus	0.883	$2.94 \times 10^5$	$2.45 \times 10^{-3}$	0.0830
Horizontal Stabilizer, HS	0.127	$4.23 \times 10^4$	$6.46 \times 10^{-3}$	0.0788
Vertical Stabilizer, VS	0.159	$5.30 \times 10^4$	$5.77 \times 10^{-3}$	0.0262

Table 3: Values of  $Re$ ,  $C_f$ , and  $S_w$  for Non-Lifting Surfaces

The drag force equation is comprised of the surface friction of the non-lifting components:

$$D_f = q(C_{f,fus}S_{w,fus} + C_{f,HS}S_{w,HS} + C_{f,VS}S_{w,VS})$$

$$D_f = \frac{1}{2}\rho U^2 S(C_{f,fus}S_{w,fus} + C_{f,HS}S_{w,HS} + C_{f,VS}S_{w,VS})$$

$$D_f = U^2 \times 0.182 \frac{kg}{m} \times 0.000863$$

$$D_f = U^2(0.000157) \frac{kg}{m}$$

### 3.2 Range versus Speed - Theory and Tests

Prior to flight day, the theoretical model predicted the range *Checkmate* would fly over varying flight speeds, indicated by the red curve below. The blue stars indicate the experimental values, plotted over the predicted curve to show the clear discrepancies.

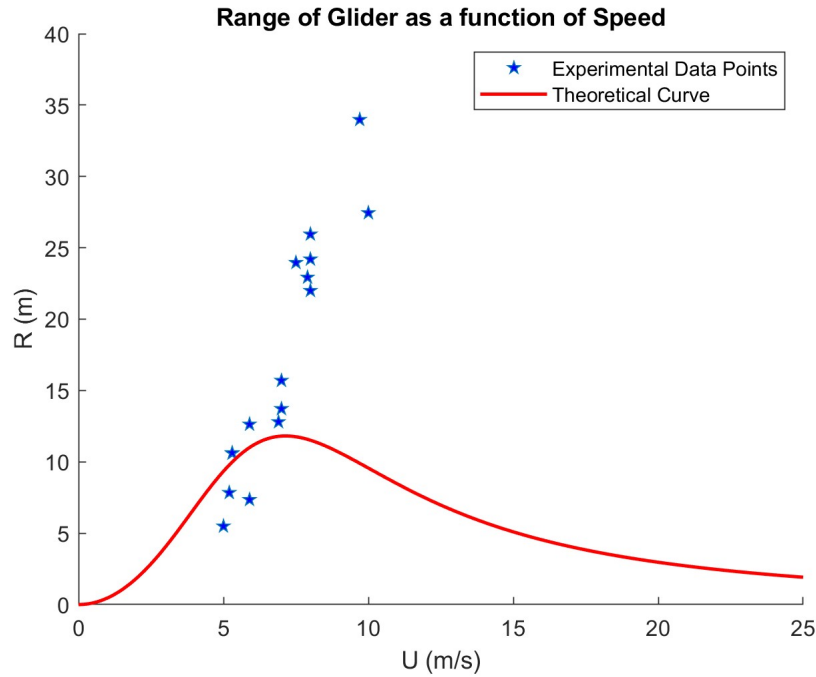


Figure 7: Predicted and Experimental Range of *Checkmate* versus  $U$

It can be seen that the experimental values seem to have a linear increase in  $R$  with increase in  $U$ , with no apparent peak value. The testing resulted in an average range  $R$  of 14.5m with a standard deviation of 2.62m. The average airspeed is 7.04 m/s and the standard deviation of airspeed is 1.54 m/s. It appears as if *Checkmate* has not been flown to the  $U$  of  $R_{max}$ .

## 4 Discussion

### 4.1 Comparison of Theory and Experiment

Assuming that the glider was gliding, there are several factors which would have led to such an erroneous prediction.

*Checkmate* would arrive at a higher maximum range at a higher speed. The curve of best fit is generated based on the tendencies of the theoretical curve.

From the derived relationships between each drag component and airspeed, the following can be concluded with Equations 4, 25, and 26:

$$D \sim U^2 + \frac{1}{U^2} \quad (27)$$

Next considering that  $R = h(\frac{L}{D})$  with constant  $h$ , the theoretical equation can be written in the same form

$$R = \frac{1}{(a)U^2 + \frac{b}{U^2}} \quad (28)$$

where:

- $a = \frac{\rho(S_{w,Fus} \times C_{F,Fus} + S_{w,HS} \times C_{F,HS} + S_{w,VS} \times C_{F,VS} + S(C_{D,min}))}{2hmg}$
- $b = \frac{2Kmg}{\rho S h}$

$\rho$ ,  $S$ , launch height, and all  $S_W$  values can be assumed to be constant.

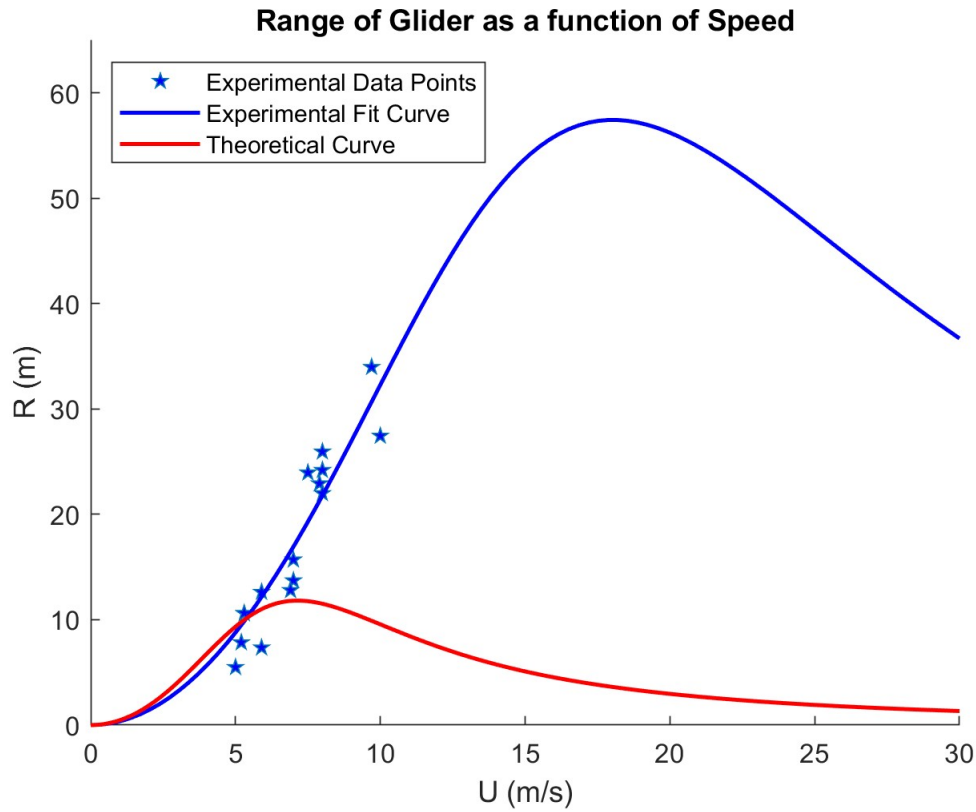


Figure 8: Predicted and Experimental Range versus  $U$  Incorporating a Fit Line

Equation 28 can be used to generate a fit line from the experimental data. The best fit equation calculated from the data points is  $R = \frac{1}{(2.68 \times 10^5)U^2 + \frac{7.58 \times 10^5}{U^2}}$ .

Many assumptions and predictions are made when calculating the line of best fit. The new curve is a tentative prediction, and is unlikely to be accurate. Instead it is used to demonstrate that the airspeed of maximum range was not reached during testing, and  $R_{max}$  is placed at a higher  $U$  than the originally predicted value.

To identify the parameter(s) in the theoretical model that cause error, several constants were altered to observe the trend in the theoretical curve. The constants selected were  $C_{D,min}$ , because it was calculated from a low Reynolds number which could cause inaccuracies in predicted aerodynamic values, and  $m$ , because the scales used had a large margin of error.

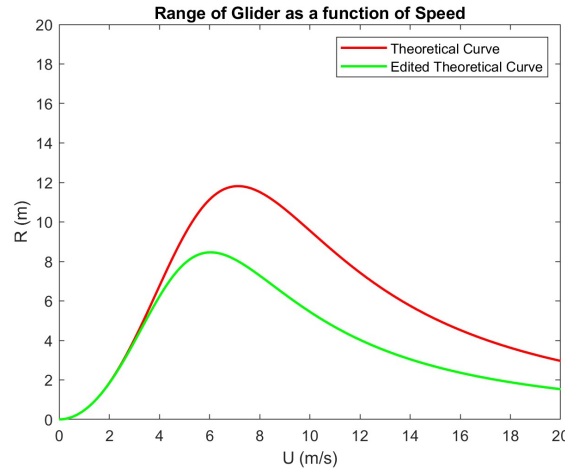


Figure 9:  $R$  versus  $U$ , Theory and Edited Theory, Doubled  $C_{D,min}$

Doubling  $c_{d,min}$  results in a proportional decrease of  $R_{max}$  by about 1/3 and shifting back by about 1/7. The real  $c_{d,min}$  could differ from the value taken from airfoiltools.com, as airfoiltools.com utilizes X-Foil to simulate the polars. The X-Foil software simulates and provides data points for inviscid flight at high Reynolds numbers. However, the simulated values for NACA6412 was at a low Reynolds number of 50,000. Therefore, the values used for  $C_D$  and  $C_L$  inputted into the theoretical prediction could be different from the real values as viscid effects could occur.

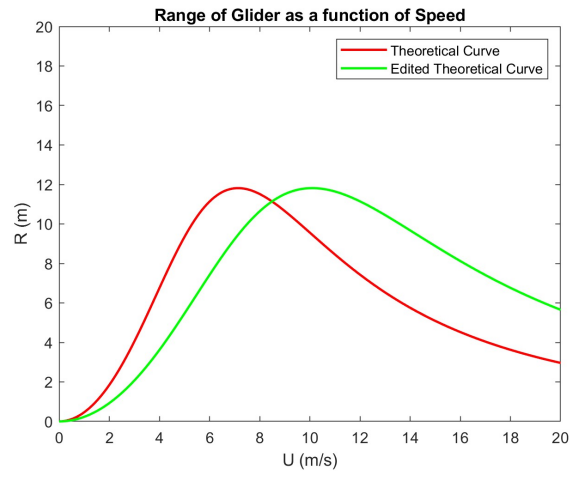


Figure 10:  $R$  versus  $U$ , Theory and Edited Theory, Doubled  $m$

Doubling glider mass  $m$  results in a proportional shifting forward of the  $U$  value of  $R_{max}$  by about  $2/5$ .

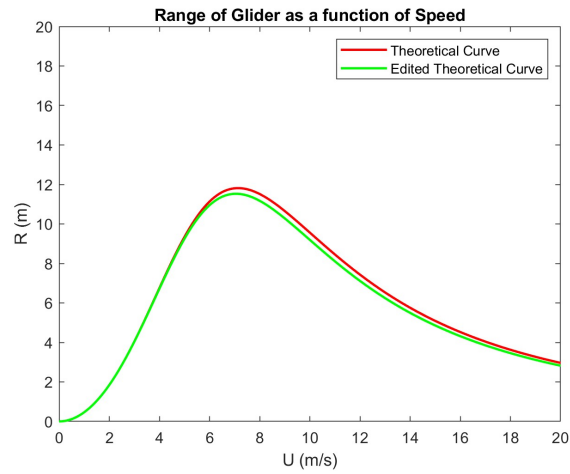


Figure 11:  $R$  versus  $U$ , Theory and Edited Theory, Doubled  $C_f$

Doubling all  $C_f$  values results in a decrease and shifting back of  $R_{max}$  with a much smaller magnitude than that of previous changes. This increase in  $C_f$  could create a similar effect to accounting for skin friction drag. However, the small change implies that  $C_f$  does not significantly affect gliding performance, regardless of differences between theoretical and experimental values.

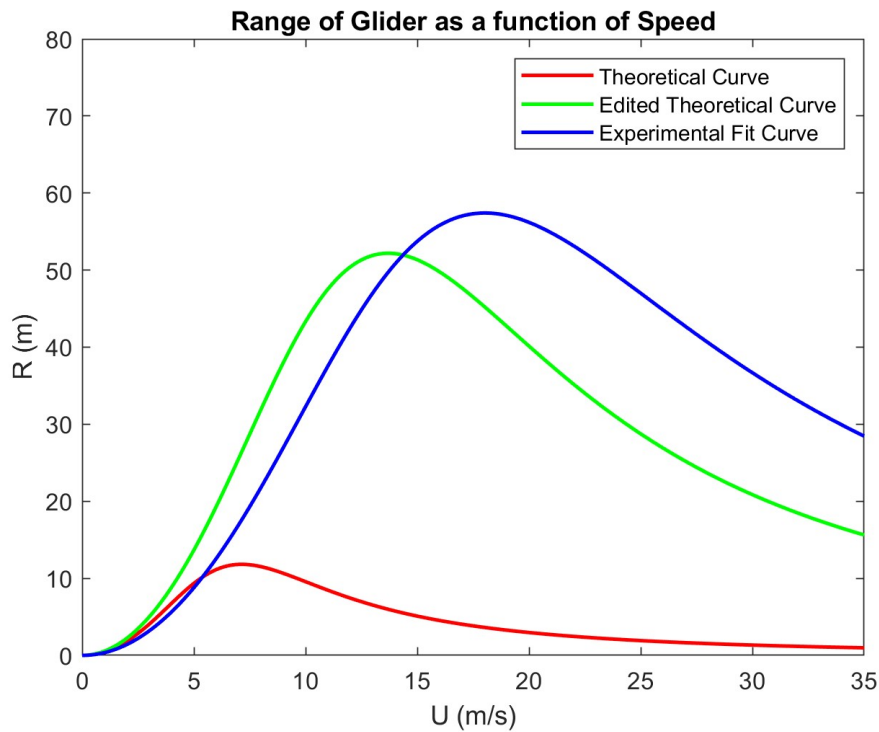


Figure 12:  $R$  versus  $U$ , Experimental Fit Line versus Theory and Edited Theory

In order for the theoretical graph to more closely resemble the experimental best fit graph, the weight must be increased slightly and the value of  $C_{D,min}$  must be decreased.

However, for the theoretical graph to be near the best fit graph in value,  $C_{D,min}$  must be decreased by a factor greater than  $10^3$ . This suggests that the best fit curve cannot be reliably obtained from the data. The curve may have been more reliable if the data points included a clear peak value.

## 4.2 Wing Loading, $W/S$

The table below shows *Checkmate's* wing loading value, alongside several other flying devices.

Flying Device	Weight, $W$ (N)	Wing Area, $S$ ( $m^2$ )	Wing Loading ( $\frac{N}{m^2}$ )
<i>Checkmate Glider</i>	8.82	0.296	29.8
Barn Swallow	0.170	0.012	14.2
Barn Owl	5.00	0.168	29.8
Black Vulture	21.0	0.330	63.6
Icaré 2 (solar-powered airplane)	3,500	21	167
Airbus A380	5,600,000	845	6,630

Table 4: Wing Loading Comparison

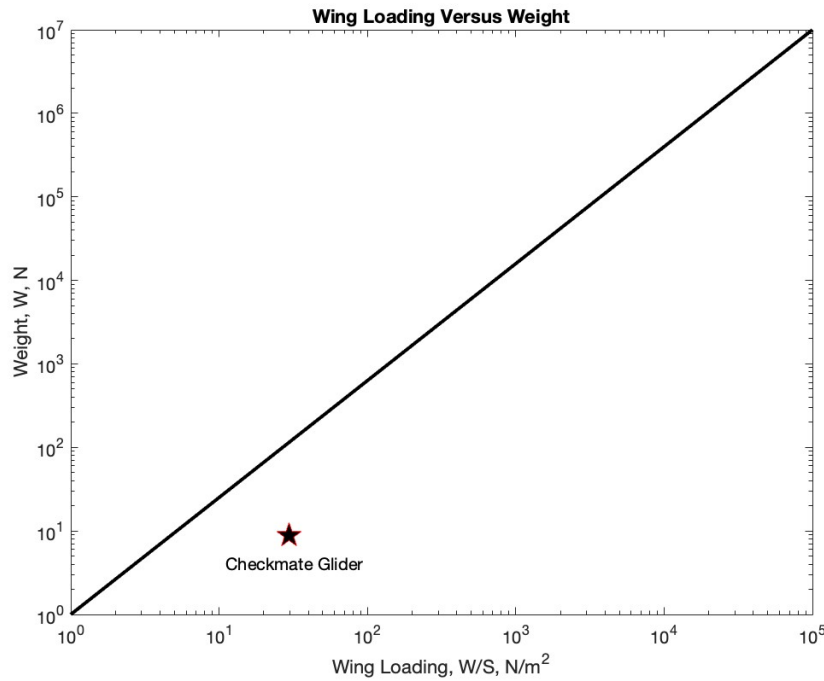


Figure 13: Predicted Weight versus Wing Loading Values

The line on the log scale graph is the predicted variation of weight vs wing loading. *Checkmate*, denoted above by the star, falls under the expected line for its weight, and therefore has a lower wing loading than anticipated.

There is a short derivation which creates a simple relationship between flight speed and wing loading. Starting with a variation of Equation 1:

$$L = \frac{1}{2} \rho U^2 C_L$$

In gliding flight,  $L \approx W$ :

$$U = \sqrt{\frac{2W}{\rho S C_L}}$$

$W$ ,  $\rho$ , and  $C_L$  are all constant in gliding flight, therefore:

$$U \sim \sqrt{\frac{W}{S}} \sim \sqrt{\text{Wing Loading}}$$

*Checkmate* features an unusually low wing loading, notably falling below the expected value for flying devices with similar weights. This characteristic enhances *Checkmate's* ability to fly at low air speeds when compared to those similarly weighted .

### 4.3 $(L/D)_{max}$

#### 4.3.1 Derivation and Calculation

The following equations will be used for the derivation.

$$\frac{L}{D} = \frac{C_L}{C_D}$$

$$C_{D,i} = KC_L^2$$

$$C_D = C_{D,o} + C_{D,i}$$

At  $(L/D)_{max}$  the condition below is true:

$$C_{D,o} = C_{D,i}$$

$$\therefore C_D = 2C_{D,o}$$

Solving for  $(L/D)_{max}$

$$C_{D,i} = C_{D,o} = KC_L^2$$

$$C_L = \sqrt{\frac{C_{D,o}}{K}}$$

$$\left(\frac{L}{D}\right)_{max} = \frac{\sqrt{\frac{C_{D,o}}{K}}}{2C_{D,o}}$$

$$\left(\frac{L}{D}\right)_{max} = \frac{1}{2\sqrt{KC_{D,o}}}$$

The  $(L/D)_{max}$  value occurs at the when  $D$  is at its minimum, where it is equal to  $D_o$ .

Equation 5 states:

$$D_0 = D_f + D_{pro}$$

Equation 8 is defined in section 3.1:

$$D_f = U^2(0.000157) \frac{kg}{m}$$

Equation 11 states:

$$D_{pro} = c_{d,min}qS$$

The  $c_{d,min}$  discussed in section 1.1 turns out to be 0.055 at  $Re = 5 \times 10^4$ .

$$D_{pro} = c_{d,min}\left(\frac{1}{2}\rho U^2 S\right)$$

$$D_{pro} = 0.055 \times U^2 \times .5 \times 1.23 \frac{kg}{m^3} \times 0.296m^2$$

$$D_{pro} = U^2(0.01) \frac{kg}{m}$$

Combining the drags yields:

$$D_0 = U^2(0.000157) + U^2(0.01) = U^2(0.0102) \frac{kg}{m}$$

As seen in the theoretical curves from part 4,  $(\frac{L}{D})_{max,theory}$  occurs at  $U \approx 7.5 \frac{m}{s}$ . Plugging U in yields:

$$D_o = 0.587N$$

$$D_o = qSC_{D,o}$$

$$C_{D,o} = \frac{D_o}{qS} = \frac{0.587}{(34.6)(0.296)} = 0.0573$$

To calculate K the aspect ratio and Oswald efficiency must be defined. AR is defined in Table 1 and  $e_v$  is defined by taking an approximation based on Appendix A of Scholz's "Estimating the Oswald Factor From Basic Aircraft Geometrical Parameters" (Source: Scholz). The selected  $e_v$  of 0.75. Using these values:

$$K = \frac{1}{\pi AR e_v} = \frac{1}{\pi(5.5)(0.75)} = 0.0772$$

By plugging both values into the equation:

$$\left(\frac{L}{D}\right)_{max,theory} = \frac{1}{2\sqrt{KC_{D,o}}} = \frac{1}{2\sqrt{(0.0772)(0.0573)}} = 7.52$$

The experimental  $(L/D)_{max}$  is found below:

$$R = h \left(\frac{L}{D}\right)$$

$$\left(\frac{L}{D}\right)_{max,exp} = \frac{R_{max}}{h} = \frac{34.0}{1.58} = 21.5$$

### 4.3.2 Comparison

$$21.5 > 7.50$$

$$\left(\frac{L}{D}\right)_{max,exp} > \left(\frac{L}{D}\right)_{max,theory}$$

## 4.4 $U_\gamma$

### 4.4.1 Prediction

The following equation describes the glide angle:

$$\begin{aligned}\tan(\gamma) &= \frac{h}{R} \\ \tan(\gamma) &= \frac{h}{h(\frac{L}{D})} \\ \tan(\gamma) &= \frac{1}{\frac{L}{D}} \\ \therefore \gamma_{min} \text{ at } \left(\frac{L}{D}\right)_{max}\end{aligned}$$

Using 4.3 and the lift equation the  $U_\gamma$  is derived:

$$\begin{aligned}U^2 &= \frac{2W}{\rho S C_L} \\ C_L &= \sqrt{\frac{C_{D,o}}{K}} \\ U_\gamma^2 &= \frac{2W}{\rho S \sqrt{\frac{C_{D,o}}{K}}} \\ U_\gamma &= \sqrt{\frac{2W}{\rho S \sqrt{\frac{C_{D,o}}{K}}}}\end{aligned}$$

By plugging in values,  $U_\gamma$  is found:

$$U_{\gamma,theory} = \sqrt{\frac{2W}{\rho S \sqrt{\frac{C_{D,o}}{K}}}} = \sqrt{\frac{2(8.83)}{(1.23)(0.296) \sqrt{\frac{(0.0573)}{(0.0772)}}}} = 7.50 m/s$$

### 4.4.2 Comparison

$$\begin{aligned}9.7 \frac{m}{s} &> 7.5 \frac{m}{s} \\ U_{\gamma,exp} &> U_{\gamma,theory}\end{aligned}$$

## 4.5 $C_L$ at $D_{min}$

### 4.5.1 Calculation

Starting with Equation 1:

$$W = qSC_L = \frac{1}{2}\rho U^2 SC_L$$

Using the  $U_\gamma$  value found above and solving for  $C_L$

$$C_{L,D_{min}} = \frac{2W}{\rho S U_\gamma^2}$$

Using Equation 3 in Section 1.1, the theoretical  $C_L$  value is calculated below:

$$C_{L,\alpha} = \frac{2\pi(AR)}{(AR) + 2} = \frac{2\pi(5.5)}{5.5 + 2} = 4.6/rad$$

This formula demonstrates a 4.6 increase in  $C_L$  per radian increase in  $\alpha$

$$m = \frac{4.6}{1rad} \times \frac{\pi rad}{180^\circ} = 0.08/degree$$

This is the slope for the  $C_L(\alpha)$  plot as  $\alpha$  is measured in degrees.

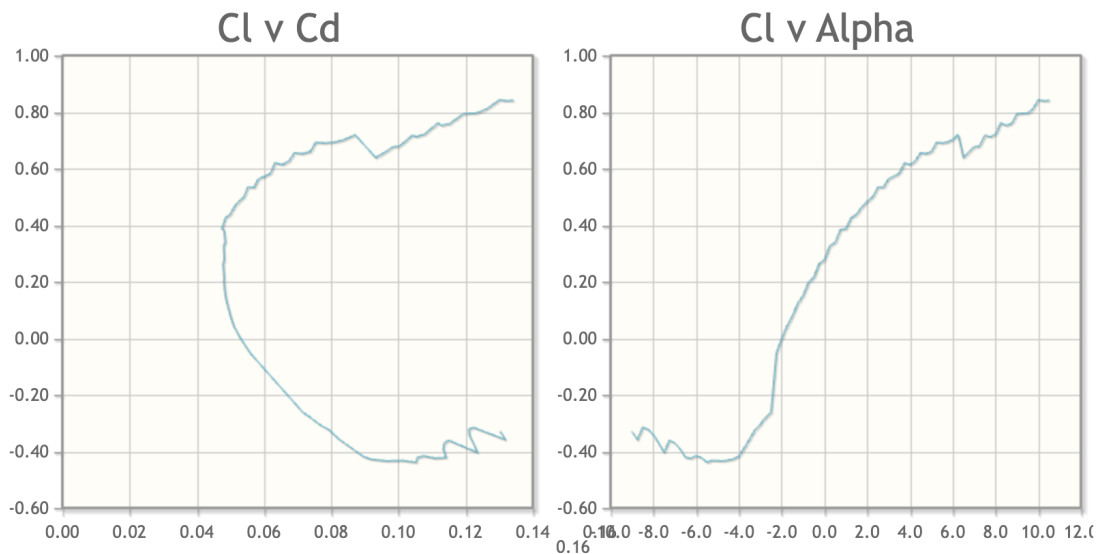


Figure 14: Airfoil Polars for NACA6412 at  $Re = 5 \times 10^4$  (Source: Airfoil Tools)

From plot:  $c_l = 0$  at  $\alpha = -2^\circ$

$$y_1 - y_2 = m(x_1 - x_2)$$

$$0 - C_L = \frac{0.08}{\text{degree}}(-2^\circ - 2^\circ)$$

$$C_L = 0.320$$

Using the values above  $C_{L,D_{min}}$  is calculated below:

$$C_{L,D_{min}} = \frac{2W}{\rho S U_\gamma^2} = \frac{2(8.83N)}{(1.23 \frac{kg}{m^3})(0.296m^2)(7.5 \frac{m}{s})^2} = 0.862$$

#### 4.5.2 Comparison

$$0.862 > 0.320$$

$$C_{L,D_{min}} > C_L$$

## 5 Summary

The glider did not perform as predicted. Section 4.1 discussed potential changes that would shift the theoretical curve to a higher U, closer to the experimental values. One of the parameters which did so was drastically decreasing the  $C_{d,min}$  value. However, the new value was unrealistically small, at around 1/1000 its original value.

Section 4.2 demonstrated the wing loading predictions through Figure 14. This figure highlights *Checkmate's* apparent over-performance at lower air speeds.

In Section 4.3 the theoretical and experimental  $(L/D)_{max}$  are vastly different from each other. The experimental values of R never peak, creating significant uncertainty. The experimental value of  $(L/D)_{max} = 21.5$  is at best a minimum, meaning the difference between theory and experiment can only increase. The maximum value of  $(L/D)_{max}$  also govern the values  $U_\gamma$  and  $C_{L,D_{min}}$ , creating even more uncertainty. Already, the two values significantly vary from their theoretical counterparts, as seen in sections 4.4 and 4.5.

The reason for a lack of peak is due to the limitations of the equipment used as the rail launch system did not launch past 10 m/s. Regardless, the theoretical predictions are still vastly different from the experiment. A possible source of the error could be due to the limitations of X-foil, as explained in Section 4.1.

When predicting the performance of a glider, various assumptions were made. The principle assumption made was that the glider glides and descends at a constant sink rate and air speed. Empirically, gliding is shown using Equation 22.

This assumption, however, does not hold true as a stall pattern was observed throughout the experiment. Stalls occur when the angle of attack of an airfoil exceeds the maximum lift value and causes the glider to fall as shown below:



Figure 15: *Checkmate* Glider Stalling on Glider Day

During Glider Day, changes were made to the glider to have a better performance, one of the changes was to increase the angle of attack of the wing. At higher speeds the increased angle of attack and  $C_L$  caused the plane to pitch up to a greater height and stall. The increase in height indicates that  $L > W$ . Therefore, the assumption of gliding flight is not met during the experimental tests as the forces are not in equilibrium, thus having a inconstant airspeed and sink rate. The model prediction does not account for these changes in flight and thus represents an inaccurate depiction.

Beyond the wing angle of attack, other unpredicted changes were made to the glider before launch. These changes were made to improve the performance of the glider based on the characteristics of the glider. One change to the glider was the adjustment of the center of mass by decreasing the amount of putty in the nose of the plane. Although the center of mass was not a factor in the prediction, this changed the mass of the glider. However, this change was minimal and does not have a vast effect on the predicted performance of the glider. Lastly, the glider tended to roll to the left, therefore, the trim was changed to negate the roll for the glider to maintain a steady flight. Overall, the changes made to the glider were not represented in the model thus the experimental results did not match the predictions.

The purpose of this report is to compare the predicted performance with the true performance of the glider. Various factors were tested to compare the performances including graphing data, manipulating equations and comparing key values. Lastly, by discussing the causes for the changes seen through these factors, the conclusion is clear that the glider did not match the predicted performance.

## 6 References

“NACA 6412 (Naca6412-II).” Airfoiltools.com, 2023, [airfoiltools.com/airfoil/details?airfoil=naca6412-il](https://airfoiltools.com/airfoil/details?airfoil=naca6412-il). Accessed 16 Nov. 2023.

Scholz, M. Nita. D. Estimating the Oswald Factor from Basic Aircraft Geometrical Parameters. 2012, [www.fzt.haw-hamburg.de/pers/Scholz/OPerA/OPerA\\_PUB\\_DLRK\\_12-09-10.pdf](http://www.fzt.haw-hamburg.de/pers/Scholz/OPerA/OPerA_PUB_DLRK_12-09-10.pdf). Accessed 16 Nov. 2023.

Spedding, Geoffrey&nbsp;R, and John McArthur. “Span Efficiencies of Wings at Low Reynolds Numbers.” Span Efficiencies of Wings at Low Reynolds Numbers, Aerospace Research Central, 22 May 2012, [arc.aiaa.org/doi/10.2514/1.44247](https://arc.aiaa.org/doi/10.2514/1.44247).

Tennekes, Henk. “The Simple Science of Flight.” Simple Science of Flight, MIT Press, 4 Sept. 2009, [users.dimi.uniud.it/~antonio.dangelo/Robotica/2012/helper/AerialRobotics/Simple\\_Science\\_of\\_Flight.pdf](https://users.dimi.uniud.it/~antonio.dangelo/Robotica/2012/helper/AerialRobotics/Simple_Science_of_Flight.pdf).

“2 x 4 plan - free download.” Outerzone, 8 April 2015, [https://outerzone.co.uk/plan\\_details.asp?ID=6544](https://outerzone.co.uk/plan_details.asp?ID=6544).



Figure 16: Magnus Carlsen Depiction on Glider